

Ion beam mixing in Ag-Pd alloys

J. L. Klatt and R. S. Averback

Department of Materials Science and Engineering, University of Illinois at Champaign-Urbana, Urbana, Illinois 61801

David Peak

Department of Physics, Union College, Schenectady, New York 12308

(Received 3 April 1989; accepted for publication 19 July 1989)

Ion beam mixing during 750 keV Kr⁺ irradiation at 80 K was measured on a series of Ag-Pd alloys using Au marker atoms. The mixing in pure Ag was the greatest and it decreased monotonically with increasing Pd content, being a factor of 10 higher in pure Ag than in pure Pd. This large difference in mixing cannot be explained by the difference in cohesion energy between Ag and Pd in the thermodynamic model of ion beam mixing proposed by Johnson *et al.* [W. L. Johnson, Y. T. Cheng, M. Van Rossum, and M-A. Nicolet, Nucl. Instrum. Methods B 7/8, 657 (1985)]. An alternative model based on local melting in the cascade is shown to account for the ion beam mixing results in Ag and Pd.

The importance of thermal spikes in low-temperature ion beam mixing (or ion mixing) has been demonstrated both experimentally and theoretically.¹⁻⁶ What is not so evident, however, are the magnitude of the thermal spike contribution to mixing, the metals in which thermal spikes are important, and the diffusion mechanisms within the thermal spike. When discussing the quantitative aspects of ion mixing, it is often convenient to refer to the ion beam mixing parameter $\langle Dt \rangle / \Phi F_D$, where $\langle Dt \rangle = 1/6 \langle R^2 \rangle$, $\langle R^2 \rangle$ is the mean square displacement per atom during the irradiation, Φ is the ion fluence, and F_D is the damage energy deposited per unit length normal to the specimen surface. As ion mixing is a stochastic process, it can be expressed as

$$\frac{\langle Dt \rangle}{\Phi F_D} = \left(\frac{\langle Dt \rangle}{\Phi F_D} \right)_{\text{coll}} + \left(\frac{\langle Dt \rangle}{\Phi F_D} \right)_{\text{thermal spike}}, \quad (1)$$

where the two terms on the right represent, respectively, the collisional and thermal spike contributions to mixing. The collisional mixing has been calculated by both Boltzmann transport theory and computer simulation using the assumptions of binary collisions and linear cascades, and a value of $(\langle Dt \rangle / \Phi F_D)_{\text{coll}} = 1-7 \text{ \AA}^5/\text{eV}$ has been obtained.^{7,8} Various treatments of thermal spike mixing have also been formulated, although that by Vineyard,⁹ as applied by Johnson *et al.*,¹ has been widely used. The model assumes that atomic jumps occur as the cascade cools with rate,

$$\frac{d\eta}{dt} = A \exp\left(\frac{-Q}{k_B T}\right), \quad (2)$$

where $k_B T$ is the product of Boltzmann's constant and temperature, A is a constant, and Q is the activation enthalpy for jumping. With assumptions of a temperature-independent specific heat c_p and thermal conductivity κ , Eq. (2) leads to the result⁹

$$\left(\frac{\langle Dt \rangle}{\Phi F_D} \right)_{\text{thermal spike}} = \frac{A\epsilon}{6\kappa c_p n_0^{5/3} Q^2}, \quad (3)$$

where ϵ is the cascade energy per unit length (assuming a cylindrical geometry) and n_0 is the atomic density. Johnson *et al.* have suggested that the cohesive energy E_{coh} of the material is the appropriate choice for Q .¹

Van Rossum *et al.* have measured ion mixing on a series

of bilayer metal specimens and have shown that the $1/E_{\text{coh}}^2$ dependence of Eq. (3) is a well obeyed for many samples, but, notably, not for their Au/Ag sample.¹⁰ Kim *et al.* measured low-temperature ion beam mixing in a series of pure metals using tracer impurity marker atoms and *also* found qualitative agreement with Eq. (3). They observed, however, that the mixing parameter of many of the refractory metals of moderate to low atomic number had the same magnitude as that deduced from collisional mixing theories, $4-8 \text{ \AA}^5/\text{eV}$, but in the noble metals and Al, it was much higher.² Recently, Ma *et al.* measured low-temperature mixing in a series of Al transition metal bilayer samples and found that some samples showed thermal spike behavior, and others, not.¹¹ The sum of these results suggests that thermal spikes play an important role in ion beam mixing, but that many basic features of ion mixing are unexplained by Eq. (3). Most surprising is that apparent discrepancies are found in the noble metals and Al, metals with low cohesive energies where the thermal spike model seems most appropriate. The current work examines why ion mixing in the noble metals and Al (and possibly others) does not fit the simple Vineyard-Johnson model.

Ion mixing was measured in a series of Ag-Pd alloys using a Au marker. This alloy system forms a single solid solution across the phase diagram. Moreover, the atomic number, crystal structure, and lattice parameter are nearly identical in Ag and Pd. The cohesive properties of the alloys, however, vary strongly with alloy composition; the melting temperature (cohesive energy) rises from 962 °C (2.96 eV) in pure Ag to 1552 °C (3.94 eV) in pure Pd. Thus, the Ag-Pd system provides an ideal system for varying the cohesive properties of a metal without affecting its structural or chemical properties. We point out that a second difference between Ag and Pd is their electronic structures, the density of states at the Fermi level in Pd being about a factor of 10 higher than in Ag. Although the electronic structure of metals is generally ignored in thermal spike models, it has been speculated that it can have profound effects in some metals.^{12,13} This possibility is not considered here, but the interested reader is referred to Ref. 12.

The alloys were prepared for these experiments by simultaneous vapor deposition of Ag and Pd in a vacuum sys-

tem operated at 3×10^{-8} Torr during film growth. One monolayer of Au was codeposited with the Pd and Ag over a layer ≈ 20 Å thick near the midplane of the specimen. This procedure avoids a discrete Au layer and minimizes marker contamination. The specimens were irradiated at 80 K with 750 keV Kr^+ . Two fluences were employed to verify that the mixing parameter was independent of fluence. The spreading of the Au marker layer was measured using *in situ* 2.5 MeV He backscattering analysis before the specimens were allowed to warm. The backscattering signals were fit to Gaussian distributions, and the ion mixing parameters were subsequently obtained using the relation

$$Dt = 1/2 (\Omega_{\text{irrad}}^2 - \Omega_{\text{unirrad}}^2). \quad (4)$$

Values of F_D were obtained from simulations using TRIM.¹⁴

Values of the mixing parameter are plotted in Fig. 1 as a function of Ag concentration. Also shown in the figure are the melting temperatures and cohesive energies of the alloys. The latter were obtained for the alloys by assuming that they form ideal solutions. In Fig. 2, the mixing parameter is plotted as a function of the square of the inverse cohesive energy showing that Eq. (3) does not fit the data. The negative intercept is contrary to Eq. (1) as collisional mixing can only be positive. These data, and those cited above, indicate that Eq. (3) does not describe mixing in nonrefractory metals and that some other mechanism is involved.

Recent computer simulations employing molecular dynamics have suggested that local melting occurs within energetic displacement cascades in Cu.^{6,15} In metals where local melting occurs, the thermally activated diffusion process characterized by Eq. (3) would be a poor approximation as diffusion in a melt is weakly temperature dependent and it drops off precipitously upon resolidification. In cases where the maximum thermal spike temperature does not far exceed T_m , the ion mixing is far more sensitive to T_m than suggested by the $1/E_{\text{coh}}^2$ dependence of Eq. (3) as we now show for the Ag-Pd system. The model for thermal spikes that we employ here is similar to that of Vineyard⁹ and others.¹⁶⁻¹⁹ The unique feature of the present calculation is the inclusion of liquid diffusion coefficients to determine mixing. These

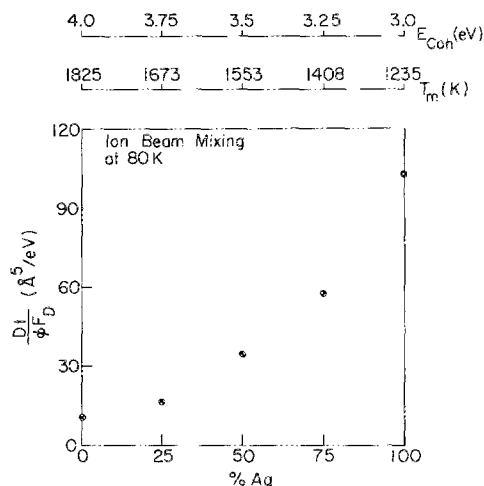


FIG. 1. Ion beam mixing parameter plotted as a function of alloy melting temperature.

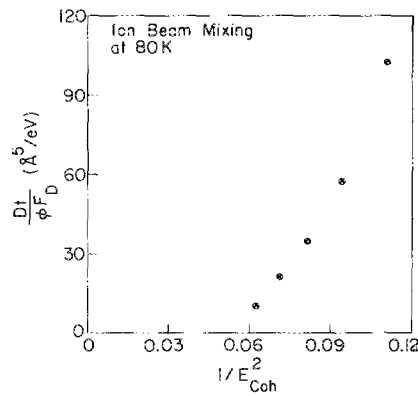


FIG. 2. Ion beam mixing parameter plotted as a function of $(1/E_{\text{coh}})^2$.

analytical models of thermal spikes are, of course, very approximate as physical parameters such as thermal conductivity and specific heat in the excited cascade are only poorly known, thermal equilibration during the cascade lifetime is only approximate, and the initial distribution of energy along the ion path is rather complicated. We treat the latter problem by assuming each primary recoil atom along the ion trajectory initiates an independent subcascade. Other details, such as electronic excitations and the latent heat of fusion, may affect quantitative aspects of the model but should not influence the qualitative features sought here. Since we are interested in comparing ion mixing in Ag and Pd, many of the approximations discussed above should cancel due to the similarity in the kinematics.

The mixing is calculated from the expression¹⁹

$$\left(\frac{\langle Dt \rangle}{\Phi F_D} \right)_{\text{thermal spike}} = \frac{1}{F_D} \int \left(\frac{d\sigma(E,P)}{dP} \right) dP \times \int n_0 V(P,t) D(P,t) dt, \quad (5)$$

where t is time, $V(P,t)$ is the instantaneous molten volume, $D(P,t)$ is the marker atom diffusion coefficient in the host melt, and n_0 is the atomic concentration. As $V(P,t)$ and $D(P,t)$ both depend on the cascade energy, the second integral over energy is included to average the results over the primary recoil spectrum. Here, $d\sigma(E,P)/dP$ is the differential cross section for a particle of energy E to produce a recoil of energy P . The damage energy is assumed to be distributed throughout the cascade volume according to

$$p_d(r) = [P_d / (2\pi\Omega^2)^{3/2}] \exp(-r^2/2\Omega^2), \quad (6)$$

where P_d is the total recoil energy. The variance Ω^2 is related to the variance in the damage energy distribution Ω^2 by $\sqrt{2\Omega^2} = (\sqrt{2\Omega^2} + r_0)$, where r_0 is assumed to be four atomic distances.²⁰ In the harmonic approximation, temperature is obtained from the relation

$$T(r,0) = p_d(r) / 3n_0 k_B. \quad (7)$$

The spike cools according to

$$\frac{\partial T}{\partial t} = \nabla \cdot (\lambda \nabla T), \quad (8)$$

where λ is the thermal diffusivity. Equation (8) is solved using the Koehler-Seitz approximation on T ,¹⁷ i.e., T is ini-

tially assumed uniform within the spherical volume $V_0 = (2\pi\Omega')^{3/2}$, with value $T_0 = 3n_0k_B P_d/V_0$; later, T remains uniform in an expanding spherical volume such that

$$V(t)T(t) = (2\pi\Omega')^{3/2}T_0. \quad (9a)$$

$T(t)$ is the solution to the temperature diffusion equation at $r = 0$.

$$T(t) = T_0(1 + t/t_c)^{-3/2}, \quad (9b)$$

where $t_c = \Omega'^2/2\lambda$. The time integral in the mixing equation becomes

$$\int (2\pi\Omega')^{3/2} \left(\frac{T_0}{T(t)}\right) n_0 D(t) dt. \quad (9c)$$

The diffusion coefficient in the melt is assumed to have the phenomenological form²¹:

$$D(T) = A(T - T_m) + B. \quad (9d)$$

Equation (9c) is solved after replacing dt by

$$dt = \frac{dt}{dT} dT = -\left(\frac{2t_c}{3T_0}\right) \left(\frac{T_0}{T}\right)^{5/3} dT. \quad (9e)$$

The results of these calculations are summarized in Tables I and II. In Table I are the ratios of the ion mixing parameters in pure Ag and Pd for different cascade energies, and in Table II are the ratios for the actual 750 keV Kr primary recoil spectrum which can be compared with experiment. Table I shows that as the cascade energy becomes large, the ratio of the mixing parameter in Ag and Pd also becomes large. This behavior is a consequence of T_0 approaching T_m in high-energy cascades in Pd and therefore to rapid resolidification and little mixing. In Table II the ratios of the mixing parameters are shown for 750 keV Kr irradiation using different cutoff energies P_{cutoff} . The cutoff energy represents the recoil energy where subcascade formation becomes important; subcascades in the present model represent distinct melts. In the calculation, recoils above the cutoff energy are assumed to have the same mixing parameter as those at the cutoff energy. For reasonable values of P_{cutoff} , 15–20 keV,²² the ratio of mixing in Ag and Pd agrees well with the experimental results. Table II also lists absolute values of the mixing parameter in pure Ag and Pd for the 20 keV cutoff energy. Unlike the ratios of the mixing parameters, these values are sensitive (approximately linear) to the choice of thermal diffusivity. For a lattice thermal diffusivity of 8×10^{13} cm² s⁻¹, the correct magnitude of mixing is obtained, providing plausibility for the model. Thus, we conclude that the phenomenon of local melting in cascades can reasonably ex-

TABLE I. Ratios of the Ag and Pd mixing parameters ξ_p for various cascade energies.

P (keV)	^a $T_{0-\text{Ag}}$ (K)	^a $T_{0-\text{Pd}}$ (K)	^b $t_{0-\text{Ag}}$ (10 ⁻¹² s)	^b $t_{0-\text{Pd}}$ (10 ⁻¹⁷ s)	ξ_p
1.0	2150	2080	0.38	0.07	10.0
4.9	3050	2850	1.60	0.64	3.4
9.8	2720	2500	2.26	0.74	4.7
14.7	2360	2150	2.50	0.52	9.0
19.6	2060	1870	2.47	0.09	71.0

^aInitial temperature in the thermal spike.

^bTime required for resolidification.

TABLE II. Ratios of the Ag and Pd mixing parameters ξ_p for different cutoff energies.

P_{cutoff}	10	15	20
ξ_p	4.4	7.5	15.9
^a $Dt/\Phi F_{D(\text{Ag})}$			75
^b $Dt/\Phi F_{D(\text{Pd})}$			5

^aUnits of keV.

^bUnits of ($\text{\AA}^5/\text{eV}$).

plain the high values of the ion beam mixing parameter in metals with low values of T_m .

In summary, these experiments have shown that the ion beam mixing parameter in a series of Ag-Pd alloys increases rapidly with increasing Ag concentration, being a factor of 10 larger for pure Ag than for pure Pd. Whereas these data do not fit the Vineyard-Johnson model for thermal spike diffusion, they are in good qualitative agreement with calculations based on a model of local melting in cascades. The reasons for the much larger ion beam mixing parameter in Ag than Pd are the larger volume and longer lifetime of the cascade melt in Ag.

This work was supported by the U. S. Department of Energy, Basic Energy Sciences, under grant DE-AC02-76ER01198.

¹W. L. Johnson, Y. T. Cheng, M. Van Rossum, and M-A. Nicolet, Nucl. Instrum. Methods B 7/8, 657 (1985).

²S.-J. Kim, M-A. Nicolet, R. S. Averback, and D. Peak, Phys. Rev. B 37, 38 (1988).

³Y. T. Cheng, M. Van Rossum, W. L. Johnson, and M-A. Nicolet, Appl. Phys. Lett. 45, 185 (1984).

⁴O. Meyer and A. Turos, Mater. Sci. Rep. 2, 371 (1987).

⁵M. W. Guinan and J. H. Kinney, J. Nucl. Mater. 103/104, 1319 (1981).

⁶T. D. de la Rubia, R. S. Averback, and R. Benedek, Phys. Rev. Lett. 59, 1930 (1987).

⁷K. Johannessen and P. Sigmund, Nucl. Instrum. Methods B 19/20, 25 (1981).

⁸W. Moller and W. Eckstein, Nucl. Instrum. Methods B 7/8, 645 (1985).

⁹G. H. Vineyard, Radiat. Eff. 29, 245 (1976).

¹⁰M. Van Rossum, Y. T. Cheng, W. L. Johnson, and M-A. Nicolet, Appl. Phys. Lett. 46, 610 (1985).

¹¹E. Ma, T. W. Workman, W. L. Johnson, and M-A. Nicolet, Appl. Phys. Lett. 54, 413 (1989).

¹²C. P. Flynn and R. S. Averback, Phys. Rev. B 38, 7118 (1988).

¹³Z. Stroubek, Appl. Phys. Lett. 45, 849 (1984).

¹⁴J. P. Biersack and L. G. Haggmark, Nucl. Instrum. Methods 174, 257 (1980).

¹⁵T. Diaz de la Rubia, R. S. Averback, R. Benedek, and H. Hsieh, J. Mater. Res. 4, 579 (1989).

¹⁶R. Kelly, Radiat. Eff. 32, 91 (1977).

¹⁷F. Seitz and J. Koehler, Solid State Phys. 2, 307 (1956).

¹⁸J. B. Sanders, Radiat. Eff. 51, 43 (1980).

¹⁹D. Peak and R. S. Averback, Nucl. Instrum. Methods B 7/8, 561 (1985).

²⁰The constant r_0 is added to the variance in the damage distribution to account for the energy leaving the cascade by supersonic processes such as focusons and replacement collision sequences. The value of four atomic distances is arbitrary.

²¹A. Bruson and M. Geri, Phys. Rev. B 19, 6123 (1979).

²²K. L. Merkle, in *Radiation Damage in Metals*, edited by N. L. Peterson and S. D. Harkness (American Society for Metals, Metals Park, OH 1976), p. 58.